THE RESISTANCE OF FIBER-REINFORCED 3D PRINTED STAB-PROOF ARMOR ELEMENTS: MATERIALS, GEOMETRIES, DIMENSION AND ORIENTATION

SITOTAW, DEREJE BERIHUN[1*]; MUENKS, DOMINIK[1] AND KYOSEV, YORDAN KOSTADINOV[2]

1   Ethiopian Institute of Textile and Fashion Technology, Bahir Dar University, Bahir Dar, Ethiopia
2   Chair of Development and Assembly of Textile Products, Institute of Textile Machinery and High Performance Material Technology, Faculty of Mechanical Science and Engineering, TU Dresden, 01069, Dresden, Germany

ABSTRACT

The majorities of stab protective armors limit several comfort parameters such as locomotion, movement, respiration, flexibility and weight which determine the efficient use by officers. Lightweight and effective protection with the necessary comfort parameters such as flexibility, respiration and free locomotion through the development of three dimensional printed (3DP) scales based on natural armors from fibers using continuous filament fabrication is the main objective of this research. In this study, stab protective armor scale-like elements with different materials, shapes, sizes and portions of a part investigated against stabbing force. Onyx, Aramid, carbon and different ratio Onyx/Kevlar by inserting fiber at different fiber filling angles $(0/45/90/135)_N$ were used in this investigation. The specimens were tested according to VPAM KDIW 2004. The result revealed that the scales with Onyx, Kevlar/Onyx and Kevlar fiber-reinforced protective scales failed while the carbon fiber resists the puncturing energy level K1 (25 J) with the penetration depth less than the maximum allowable penetration depth of the knife through the protectors. The large size protective elements and rectangular geometries withstand the impact energy relative to triangular geometries. The result revealed that the material type, its alignment, size and shapes of protection elements and portions of the scales where the weight dropped significantly influence the resistance against the impact energy to puncture with the intended energy level and sharp tipped knife.

KEYWORDS

Protection armor; 3D printed scales; Impact energy; Penetration depth; Fiber-reinforcement; Geometries and their sizes; 3D printing; Stab protection.

INTRODUCTION

Protective clothing is one of the most important pieces of safety equipment to save lives. A stab resistant vest is a reinforced piece of body armor designed to resist knife or needle attacks specifically to the upper part of the body (chest, back and sides) and it can be worn either as covert or overt.

Early humans used comparatively primitive armors which were manufactured out of metal, horn, wood or leather lamellae [1] [2] but as civilizations evolved and knowledge advanced, body armor introduced. Then in the last century, with its two world wars, various attempts were made to advance the technology of body armor [1]. It was reported that the first soft body armor was developed by the Japanese and in that instance, was made of silk and was most effective against low-velocity bullets [3]. Thus the first so-called bullet-proof vests were designed in America in the two decades following World War I [4] [5] while the

modern police body armor was introduced into practice in the 1970s [6].

Security officers are stabbed everywhere during their duty shift and most of the stabbed officers are killed immediately after stabbing by the suspected assailants. As the news and reports showed that the number of stabbed officers increased from year to year in developed countries, for example, in United states of America, Germany, United Kingdom, but the stabbing frequency is more in developing, Saharan and sub Saharan countries [7-15]. The main reason for fatal injury is the officer's negligence to wear protective armor vest during their duty shift because most armor vests are heavy, non-permeable and reluctant mode of the officers. With all these limitations of most of the current armor vests police officers, military, transport and correction administrators should encourage their staffs to wear stab vests during the whole duty shift to save them from a fatal injury if stabbed in torso [16]. Armor vests

---

*   **Corresponding author:** Sitotaw, D.B., e-mail: *dere96@yahoo.com*

might not be universal but has to be designed according to the level of protection, type of weapons and techniques of stabbing by assailants in the region with the desired comfort. The level of protection required in soft and sensitive bodily regions is determined by the type of attacks that are likely to be encountered [17]. The design of appropriate stab vests with the desired level of protection can be challenging for a wide range of weapons which are used for puncture and the stabbing techniques are different depending on assailants [18].

Though protection and comfort are conflicting, body armors for stab protection should also consider [19] flexibility and other ergonomic issues for acceptance along with coverage and duration [20-22].

The selection of advanced materials (both for performance and comfort) and appropriate armor design should ideally allow the flow of excessive metabolic heat away from the body (thermo-physiological property) which can be reflected by a combination of air permeability, thermal resistance, and moisture evaporation [23-25]. The garment should be able to transfer heat and moisture away from the skin to the atmosphere [25-27]. Tactile comfort, the feel or sensation on the skin when worn should be considered during design of protection gear [28] [29].

The use of body armor has always been an issue when ease of body movement and cognitive functions are considered [30, 31] and should not be drastically compromised by the design of the body armor [22]. Many biological systems possess hierarchical and fractal-like interfaces and joint structures that bear and transmit loads, absorb energy, resist puncture and accommodate growth, respiration and/or locomotion [32], which are determined by their geometry [33-35]. In the case of bio-inspired flexible protection, natural segmented armors from fish, alligator, snake, tonicella marmoreal, pangolin, scaly foot gastropods, arapaima or armadillos are attracting an increasing amount of attention because of their unique and highly efficient protective systems to resist mechanical threats from predation, while combining hardness, flexibility, breathability, thinness, puncture-resistance and lightweight [35-40]. These natural armors, which inspired researchers because of their diversity of geometrically structured interfaces and joints, are found in biology, for example in armored exoskeletons [41] [42], the cranium [33] [34], the turtle carapace [43] and algae [44].

Learning by imitation and further by linking all the data has probably been one of the most fruitful ways of development ever used. The extreme contrast of stiffness between hard scales and surrounding soft tissues gives rise to unusual and attractive mechanisms, which now serve as models for the design of bio-inspired armors. Despite this growing interest, there is little guideline for the choice of materials, optimum thickness, size, shape and arrangement for the protective scales [45].

The performance of 3D printed aramid FRP for stab resistance was studied for 2 mm, 4 mm and 6 mm thickness and the last two showed excellent performance for 25 J impact energy while 2 mm thick scales failed the puncturing test [46]. In this research, the scales are designed, developed and its performance is checked for energy level K1 (25 J) with a relatively low thickness, mass, production time and material usage as compared to the previous research result.

The aim of this research is to design and develop three dimensional (3D) printed stab resistant armor vest based on continuous filament fabrication (CFF) inspired by natural armors. The plan is to combine soft textile undergarment and hard stab protective elements in terms of fiber-reinforced plastic (FRP) of segmented scales. As a first step for the development of innovative stab protection clothing, the stab protection properties of 3D printed and fiber-reinforced functional elements are investigated based on material types, shape of the geometries of the scales and size of geometries, which are used for the development of a novel vest. The main novelty of this research is its comfort as studied and published in a reputable journal [47] by the same authors to this article. The comfort is found to be improved as compared to the current stab protective armor because the armor's protective elements in this research are segmented scales [47] without compromising the protection performance for the intended energy level, as investigated in this research in terms of material types and its alignment during 3D printing, geometry and size.

MATERIALS AND METHODS

Materials

3D printed stab protective elements in this research are produced as circular, quadrilateral and triangular scales with defined dimensions from thermoplastic composite filament (Onyx) and functional fibers such as Kevlar from aramid groups and carbon fibers with the mechanical properties shown in Table 1. Different blend layers ratio of fibers and plastics are used in Markforged Inc.'s Mark Two Desktop 3D printer [48] with its CFF process and two printing nozzles. One nozzle of the printer operates like a typical extrusion process to lay down a plastic filament that forms the outer shell and the internal matrix of the part. The second nozzle deposits a continuous strand of composite fibers such that carbon, Kevlar, glass and others on every defined layer [49] [50] inside a conventional fused filament fabrication (FFF) thermoplastic part [51].

The specimens were sliced at 0/45/90/-45 degrees of infill angles, with defined repetitions written as a subscript after the last bracket (see Table 2), using

Table 1. Mechanical properties of materials [48].

Properties	Onyx	Carbon	Kevlar
Tensile strength (MPa)	37	800	610
Tensile modulus (GPa)	2.4	60	27
Flexural strength (MPa)	71	540	240
Flexural Modulus (GPa)	3	51	26
Compressive strength (MPa)		420	130
Compressive modulus (GPa)		62	25
Density (g/cm^3)	1.2	1.4	1.2

(Association of Test Laboratories for Bullet Resistant Materials and Constructions, 2011)

Table 2. Materials arrangement inside the 3D printed scales.

No.	Material	Fiber angle (in degree-°) coding	Filling fiber layers over the total layer	Dimension	Shape
1	Onyx	No fiber		3 mm thickness and 50 mm diameter	Circular
2	50% Onyx/50%Aramid	(0/+45/90/-45)$_3$/0/45/90	15/30 = 50.00%		
3	27%Onyx/73Aramid	(0/+45/90/-45)$_5$/0/45	22/30 =73.33%		
4	Aramid	(0/+45/90/-45)$_7$	28/30 =93.33%		
5	Carbon	(0/+45/90/-45)$_5$/0/45	22/24 =91.67%		
6	Carbon	0/+45/90/-45	24/32 = 75%	100 mm x 100 mm x 4 mm	Quadrilateral plate
7			24/32 = 75%		Quadrilateral scales
8			24.59%		Triangular scales

Eiger.io online software by Markforged Inc. Table 2 displays the material arrangement, design, and setup of the printing process to determine the optimum protective scales with the minimum possible thickness for Energy Level 1, which is 25 joules and a 20mm allowable deformation depth [52] of the knife through the 3D printed protective element. The materials and their arrangement in the 3D printed scales are shown in Table 2. The material ratio, expressed in percent (%), is based on the number of layers of reinforcing fibers relative to the layers of the whole part, but not the material volume, because the material volume depends on the density of the materials per unit volume of the geometry. The remaining layers, not shown in some of the rows in Table 2, are made from Onyx.

Methods

The development of 3D printed scales begins with designing, followed by STL file generation in Autodesk Fusion 360 software. The generated STL file is then imported into Markforged Inc.'s online slicing software called "Eiger.io" to select the type of material, assign alignment composition for each layer of the final product, and arrange the materials accordingly before being transferred to the 3D printer. The samples used for this study are 3D printed from the materials listed in Table 1, with each sample having a specific ratio and filling alignment without symmetry.

The scales are designed to have a thickness of 3 mm and a diameter of 50 mm for material investigation.

Additionally, various dimensions are explored, including quadrilateral scales with a thickness of 4 mm, triangular scales, and a square plate measuring 100 mm x 100 mm x 4 mm, for shape and size investigation. The designs of the target samples are illustrated in Figure 1A to Figure 1D, along with their corresponding standard triangle language (STL) files (Figure 1E) generated from Fusion 360.

Figure 2 illustrates the material arrangement of every layer in the 3D printed scales. The layers are arranged with different material filling angles to potentially enhance protection while reducing the overall weight of the armor element (scales). The fiber angle coding follows the standard lamination theory for composite part production. To clarify the arrangement, for example, (0/+45/90/-45)N signifies that a reinforcement fiber is printed N times sequentially in the 0, +45, 90, and -45 filling angles to complete the construction. The repetition (N) of the print layers angle is determined by the fiber diameter. For instance, a carbon fiber with a diameter of 0.125 mm is printed approximately $N = 5.5$ times for the mentioned reinforcement fiber angles, while a Kevlar fiber from the aramid group with a diameter of 0.1 mm is printed approximately $N = 7$ times for the mentioned fiber angles arrangement. The first and last layers default to thermoplastic materials, which in this study is Onyx.

Four specimens are produced, and three of them are tested for each sample following the test method of the Association of Test Centers for Anti-attack Materials and Constructions [52].
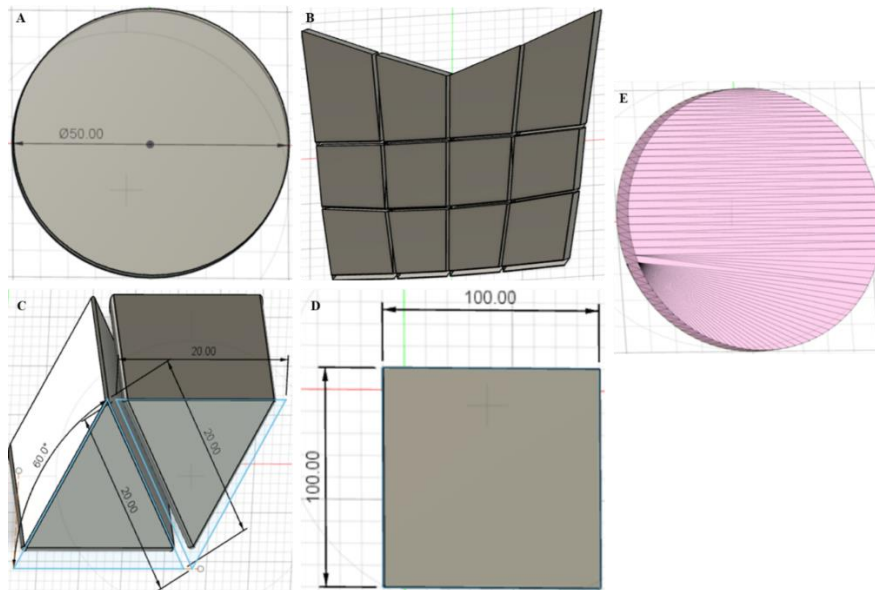
Figure 1. Designs generated from Fusion 360 A) Circular scale 3mm thick B) Quadrilateral scales 4mm thick C) Triangular scales 4mm thick D) Square plate 4mm thick E) STL file.
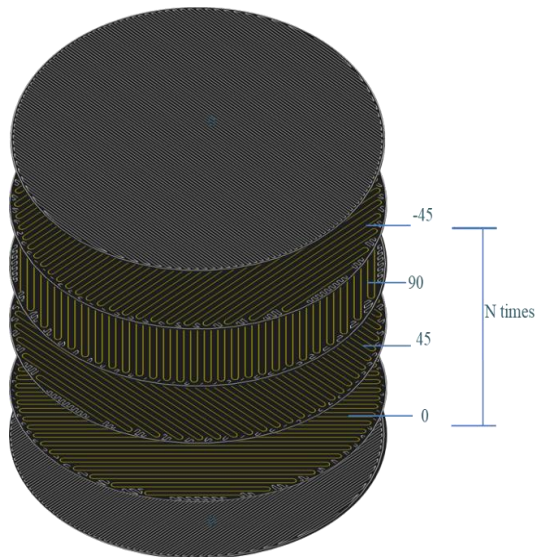

Figure 2. An example of material arrangement and printing order of polymers at filling angle (0/+45/90/-45)$_N$, generated from Eiger.io.

Experimental

The specimens are conditioned for a minimum duration of 24 hours at a temperature of 20 ± 2 °C and a relative humidity of 65 ± 5% [52]. The testing knife (blade), with specifications shown in Figure 3, is attached to the drop stand to test the resistance to puncture of the 3D printed scale-like armor elements. The dropping object, depicted in Figure 4a with the knife in Figure 4c, has a drop mass (*m*) of 2.51 kg, dropped from a height of 1.02 m at a speed (*v*) of 4.44 m/s, which is measured using an optical sensor to calculate the velocity right before impact. The kinetic energy (*E$_{kin}$*) applied to test the protection level of the specimens can therefore be calculated as follows:

$$E_{kin} = \frac{1}{2}m * v^2 = \frac{1}{2}2.51\ kg * (4.47\ \tfrac{m}{s})^2 = 25.07\ J$$

The kinetic energy used to test the specimens is 25.07 J, which is nearly identical to the specified energy in the corresponding inspection norm (K1=25 J) [52]. This energy level serves as an indicator of the specimen's protective performance, provided that the penetration depth does not exceed the standard allowable depth outlined in the norm.

The testing procedures in this study involve applying impact energy to the specimens to puncture and evaluate the performance of the armor scales against this energy. This process primarily consists of three steps: preparation of the testing setup (depicted in Figure 4, Figure 5A, and Figure 5B), puncture testing (Figure 5C), and measurement of the penetration depth (Figure 5E).

The dropping object is released from the suspension bar by pulling the rope with the holding hooked rod, causing the knife with the dropping weight to fall onto the 3D printed sample in a closed chamber (as shown in Figure 5C). Afterward, the dropped object, along with the impacted specimen, is removed from the plastiline box to measure the penetration depth of the testing knife through the scales (as illustrated in Figure 5E).

The relative alignment of the knife to the specimen with respect to the fiber filling angles (0/+45/90/-45)*N* is random for all specimens, but the center of each scale of the specimens is aligned relative to the tip of the knife to avoid deflection of the specimen upon impact. Additionally, specimens with segmented scales and single plate protective elements are subjected to multiple drop tests at different parts of a sample made from carbon fiber reinforcement.
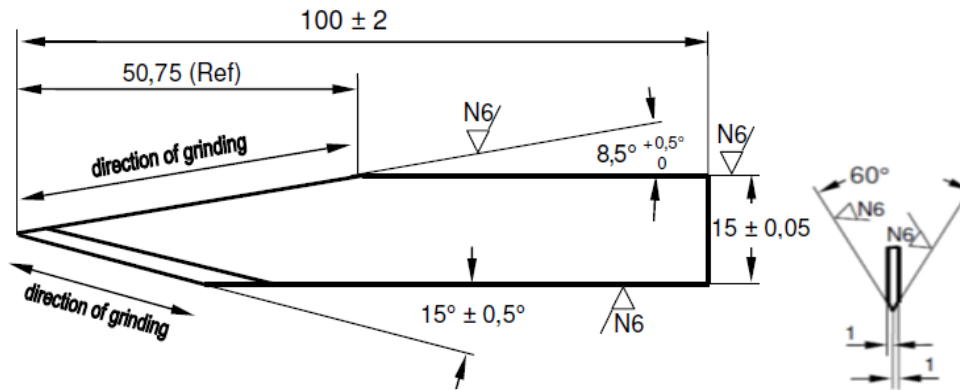
Figure 3. Geometry of the test blade P1/B (dimensions in mm) [52].
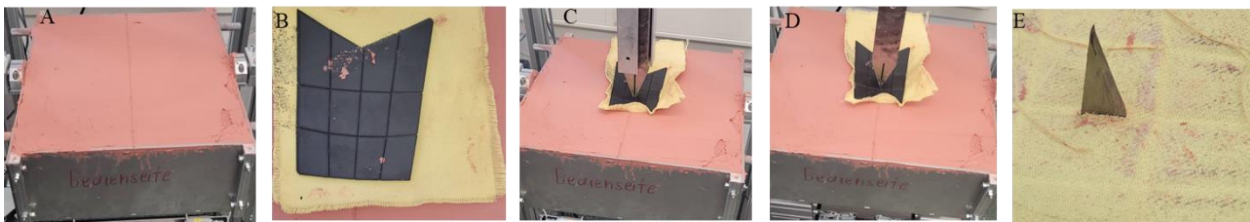

Figure 5. Test procedure of stab resistant scales using drop stand A) Leveling and center line of the plastiline B) Sample on the plastiline C) Dropped the knife with the weight D) Impacted object right after dropping E) dismantled the knife from the dropping object and measuring of the penetration depth of the knife.

Figure 4. Drop test stand with: a) Dropping weight b) Dropping weight fixing hook c) Knife d) Safety path e) Hook pulling rope f) Safety bar g) Specimen of plastiline h) Plastiline.

RESULTS AND DISCUSSION

As indicated in research results, the minimum organ distance from skin is pleura 22 mm, pericardium 31 mm, spleen 23 mm, kidney 37 mm, thoracic aorta 64 mm, abdominal aorta 87 mm [53] and liver 22 mm [54, 55]. The maximum penetration depth of the knife should be lower than the minimum distance of the organ from the skin. On the other side, the maximum penetration depth of the knife for energy level K1 (25 J) set by VPAM standard is 20 mm [52]. If the specimens allow the knife to penetrate deeper than the penetration depth set in the norm, then the samples are considered as failed to resist the specified impact energy level K1. As seen from Figure 6A - Figure 6E, the scales have shown different depths of the knife penetrated through the 3DP protective armor elements because of the type of reinforcement fibers, the fiber contents in the plates, the size of the scales and the shape of the scales.

As shown in Table 3, the influence of materials on the stab resistance at the intended energy level is investigated using various compositions: Onyx/Aramid (50% each), Onyx-27%/Aramid-73%, Kevlar-100%, Carbon-100%, and Onyx-100%. According to the test results, 50 mm diameter 3D printed carbon scales showed potential resistance against stabbing with a knife dropped at 25 joules of energy level 1. However, other materials investigated in this research demonstrated the worst potential against the same intended impact energy, resulting in fatal injury if used to develop protective armor with a 3 mm thickness and without symmetry of material

alignment during the 3D printing process. Carbon 3D printed scales do not allow the sharp tip of the knife to pass through, even for fractions of millimeters after the last layer of the 3DP protective scale, but the knife tip is deformed at every test.

The knife with the impact weight dropped on the 3D printed Kevlar scales fully passed through the plastiline with no resistance from the scale when it went through each of the aramid fiber layers. The main reason for this is the physical and mechanical properties of the materials, where the impact energy has a compression effect at first, then tensile and flexural effects. This means when an impact load is dropped on a specimen, it compresses the area, stretches it, and then deforms it. The material with the highest values for these parameters can relatively have high resistance against the intended impact energy. Carbon, with its 0.125 mm diameter, has the highest density, tensile, compression, and flexural strength and modulus (see Table 1), thus achieving the highest resistance against the intended impact energy.

The percentage of Onyx in the protective scales has no positive influence on resistance to the intended impact energy. Therefore, specimens with 3 mm thickness made from 100% Onyx and Kevlar from aramid fibers filled in the (0/45/90/-45)7 degrees

throughout the specimen have little to no resistance to puncturing because the penetration distance (>40 mm) is deeper than allowable within the testing standard [52]. Therefore, the analysis mainly focuses on the carbon and the Kevlar aramid fibers. Therefore, the analysis mainly focuses on carbon and Kevlar aramid fibers. The carbon fiber (Figure 6A) does not allow the tip of the knife to be seen behind the scale, even with fractions of a millimeter, while 100% Kevlar allows the knife to penetrate through the specimen without resistance to the impact energy (Figure 6B).

However, Kevlar with symmetry of material alignment (Figure 7) during printing showed potential resistance to the intended impact energy [56]. As the researchers reported in their paper, the symmetry of material alignment has a significant influence on the resistance to impact energy for stab protective armor. With this, Kevlar can withstand the intended impact energy when a 3 mm thickness of the scale is 3D printed with mirroring the other half thickness of the scale because half of the directions of the fiber alignment are totally opposite to the alignment of the other half fiber layers so that the running speed of the knife is disturbed during stabbing, resulting in low penetration depth.
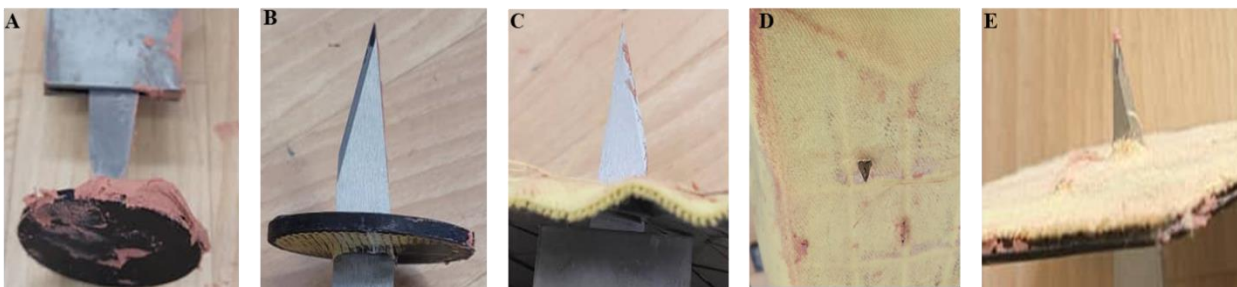

Figure 6. Appearance of scales right after impact; A) Carbon circular scale; B) Kevlar circular; C) Triangular plates; D) Quadrilateral scales on textiles E) Rectangular Plate.
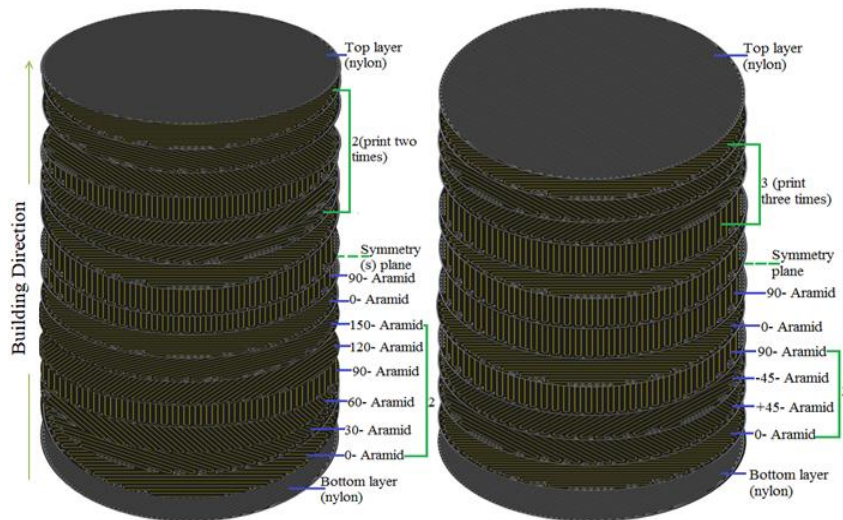

Figure 7. Example of material arrangement and printing order of aramid layers- at filling angles [(0/30/60/90/120/150)2/0/90]$_s$ and [(0/+45/90/-45)3/0/90]s, generated by Eiger.io o[56].

Table 3. Results of stab testing of FRP elements.

	Test runs	Penetration of knife in mm	Depth of plastiline deformation	Thickness	Plastic volume	Fiber Volume
Onyx/Aramid (50%)	1	44.86	16.61	3	3.9	2.12
	2	45.7	17.5	3	3.9	2.12
	3	46.21	20.45	3	3.9	2.12
	Average	45.59				
Onyx-27%/Aramid-73%	1	45.68	14.3	3	2.05	3.89
	2	46.22	18.37			
	3	43.18	15.07			
	Average	45.03				
Kevlar-100%	1	45.6	37.54	3	1.39	4.8
	2	42.25	41.12			
	3	39.45	53.43			
	Average	42.43				
Carbon-100%	1	0	64	3	1.46	4.53
	2	0	63.09			
	3	0	64.48			
	Average	0				
Onyx-100%	1	>48,5		3	5.81	
	2	>48,5				
	3	>48,5				
	Average	>48.50				
100x100mm Square Onyx-Carbon	1	20.65		4	11.92	26.79
	2	9.24				
	3	18.62				
	Average	16.17				
Quadrilateral Segments attached on textiles	1	30.63	No significant	4	17.83	24.46
	2	13.47				
	3	23.88				
	4	41.53				
	Average	27.38				
Triangular segments attached on textiles	1	41.93	No significant	4	38.24	12.47
	2	42.17				
	3	40.14				
	Average	41.41				

Figure 8 presents the 3D printed protective scales immediately after being impacted by the knife with the drop weight. The carbon fiber 3D printed protective armor element demonstrates extreme resistance to the intended stabbing energy from the drop weight. As seen from left to right in Figure 8A, the protection is perfect due to the carbon fiber's resistive reaction to the impact energy. The tips of the knives are bent, broken, and damaged in every cycle of the drop test on carbon fiber 3D printed scales (See Figure 11A to Figure 11C).

In contrast to this, the Kevlar 3D printed protective armor elements totally failed to save the wearer from fatal injury. As one views from left to right in Figure 8B, the viewer is shocked by the penetration depth of the knife through the scales because the Kevlar filaments are not able to resist the intended impact energy to puncture with the current infill angle alignment unless produced with symmetrical

alignment for half of the thickness of a scale at $[(0/+45/90/-45)3/0/90]_s$ so that the penetration depth is reduced because each layer crosses over the other layer either diagonally or at a right angle to disturb the downward running of the stabbing knife with the impact load [56].

In addition to the materials, the shapes of the protective elements also have a significant influence on the penetration depth of the knife from the impact energy. The content of the reinforcement carbon fiber in triangular scales is lower than the content in the quadrilateral scales. Figure 9 presents the running distance and turning edges because the shapes of the geometries have a significant influence on the content of the fibers (blue lines in Figure 9A and Figure 9B) to be accumulated during printing. As viewed from Figure 9A, the impact load with the knife is not able to fully penetrate after puncture and saved the wearer from fatal injury with reduced penetration

Figure 8. Physical appearance of the 3D printed scales right after impacting drop weight on A) Carbon fiber B) Kevlar fiber from aramid group.
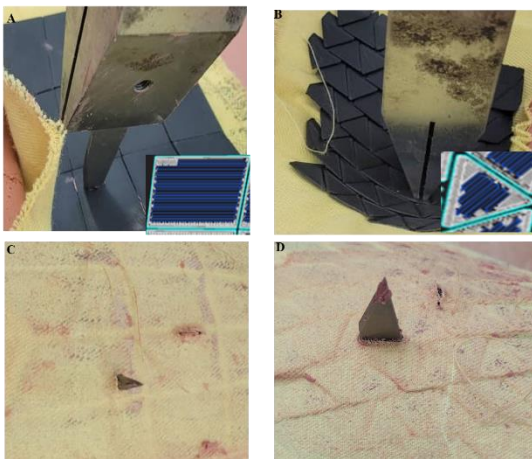

Figure 9. Appearance of the impact of drop knife on A) Quadrilateral scales B) Triangular scales and the penetration depth of knife through C) Quadrilateral D) Triangular scales.
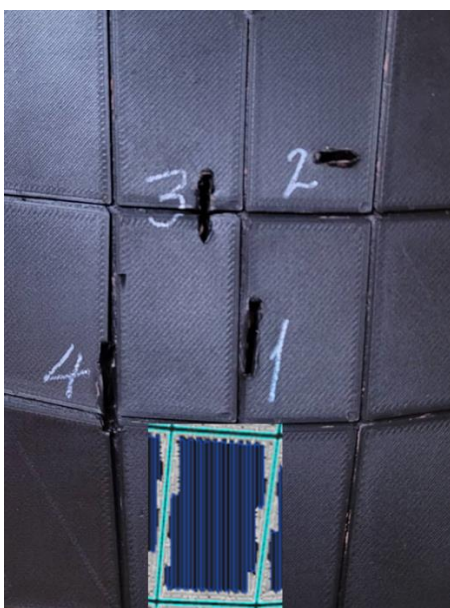

Figure 10. Appearance of the different parts of the scale right after puncture on the body (2), on the edges and joints (1, 3 and 4) of the protective elements.

depth (see Figure 9C). In contrast to quadrilateral geometries, triangular geometries allow the stabbing force with the knife to fully pass through the scales (Figure 9B) and result in fatal injury due to the shocking penetration depth of the knife (Figure 9D).

Another parameter investigated in this research is the size of the protective scales and its impact on resistance performance to stab impact energy. The size of the protective element refers to its surface area, classified as large (10,000 mm^2), medium (950-1,280 mm^2), and small size (640-750 mm^2) in this study. The large scale exhibited a penetration depth of 9.24 mm - 19.08 mm, the medium scale showed a penetration depth of 13.47 mm - 23.88 mm, and the small scales had a penetration depth greater than 30.63 mm observed during the experiment. The results showed that the sizes of the protective elements significantly influence the performance against puncture to penetrate through the scales (see Figure 6C and Figure 6E) due to the impact energy. The protection performance decreased as the dimensions of the scale became smaller. The difference in protection performance between the large scale and the small scale is akin to a saved life from fatal injury and life lost with fatal injury from the intended impact energy, according to standards and the minimum distance of sensitive organs from the skin [52-55]. The large size protective element bent the testing knife during the experiment, but the other sizes did not create physical damage to the testing knife. Previous research has revealed that the size of the protective element has an inverse relationship with comfort but is directly proportional to protection performance [56] [57] so optimization of comfort must be made without influencing protection performance.

The protection performance of the 3D printed scales also varies at different portions such as edges, joints, and the body of the protective element. As shown in Figure 10, a narrow puncture width is observed on the body (2), while a wider puncture hole is seen on the
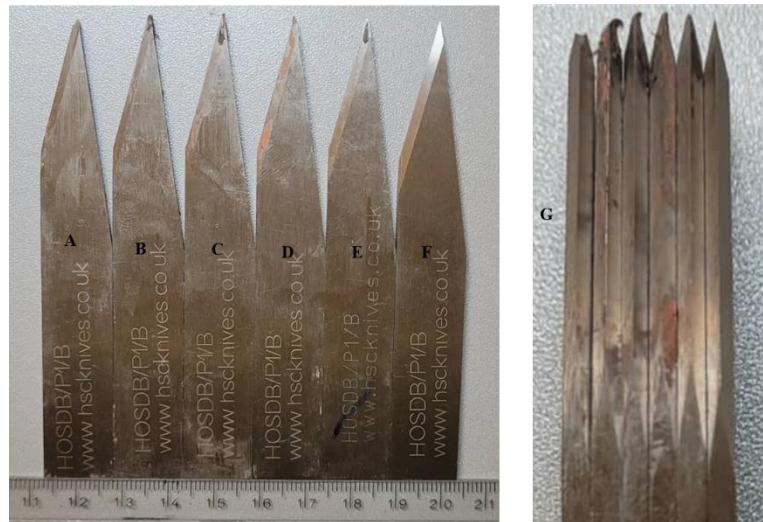
Figure 11. Damaged tip of the testing knife after impact.

edges and joints (1, 3, and 4) of the protective elements due to less fiber accumulation of the scales in edges and joint lines. The puncture width on the edges of the scales could lead to fatal injury unless improvements are made to the chamfered line in the joints of the protective elements for uniform distribution of the fibers in all parts of the scales, including the edges.

In summary, the knives are bent (Figure 10A – Figure 10E) after puncture testing and are not used to puncture repeatedly due to the high strength of the scales printed from carbon fiber in circular scales, quadrilateral scales on its body, and a 100 x 100 mm2 plate. The tips of the knives are broken, bent, or partially damaged during the drop test, according to the content of the carbon fiber in the scales. The knives in Figure 10A – Figure 10C are bent, damaged, and broken during the testing of circular scales made of carbon fiber. A knife in Figure 10D is bent during the testing of the 100 mm x 100 mm square plate, the tip of the knife in Figure 10E is bent during the testing of the body of the quadrilateral scales, while the physical appearance of the knife in Figure 10F remains unchanged during testing of the scales made from Kevlar fiber. The appearance of the tips of the knives in decreasing damage order from left to right is clearly shown in Figure 10G, with the first three knives impacted during testing carbon 3D printed scales, the fourth knife during testing of the 100 mm x 100 mm square plate, the fifth knife during the testing of the quadrilateral scales, and the last (on the right side) knife used during the testing of the circular scale made from Kevlar.

CONCLUSION

Stab protective armor is safety equipment designed to safeguard the lives of law enforcement workers for security assurance. This equipment should be capable of withstanding the intended stabbing impact energy level. This research primarily addresses the performance of continuous filament fabrication (CFF) 3D printed stab protective gear elements, considering various important factors such as the type of materials, shape of geometries, sizes of the protective elements, and related aspects. The results reveal that these considered factors significantly influence the ability to withstand stabbing impact energy from a knife with a drop weight.

The mechanical properties of materials, such as tensile strength (MPa), flexural strength (MPa), compressive strength (MPa), and their modulus (GPa), result in significantly different resistance to puncture force. Similarly, the density of the materials also plays a significant role in reducing the impact energy from the stabbing weight.

The types of geometries, described as shapes of protective scales in this study, were found to affect the penetration distance of the knife through the 3D printed protective elements because the turning point of the printer nozzle after running to print depends on the width of the printing line. The narrower the angle of the turning points of the nozzle, the lower the fiber accumulation. The sizes of the geometries influence the fiber content and affect the protection performance. The larger the geometry, the higher the fiber content, resulting in improved resistance to knife penetration through the protective element.

In general, the 3 mm thicker carbon fiber 3D printed protective scales fully resist the impact energy from the 25 joules drop weight. The tip of the knife was not measurable behind the last layer during all impact tests on carbon scales; instead, the tip of the knife is bent, broken, or damaged. Therefore, the investigators of this research suggest developing stab protective armor through 3D printing of quadrilateral scales from carbon fiber with optimal dimensions for reduced weight, flexibility, permeability, and breathability. The novelty of this study can be

explained in terms of materials mechanics as the fibers adhered to each other with crossing alignment when printing a layer over the layer. This creates an entangling path on the knife while running from layer to layer so as the impact energy is reduced by disturbing the falling speeding of the knife with its impact mass. These stab protective elements are designed for segmented arrangement for the possible flexibility with light weight from the thickness and material mechanics.

Future research activities will include the attachment method and adhesion between scales and fabrics, as well as the design and development of 3D printed scales for the full vest, and checking its performance both to protection and comfort.

REFERENCES

1. Reiners P.: Investigation about the stab resistance of textile structures, methods for their testing and improvements. Université de Haute Alsace: HAL. 2016, pp. 195.
2. Fenne P.: Protection against knives and other weapons. Textiles for protection, ed. R.A. Scott. 2005, Cambridge: Woodhead Publishing, CRC.
3. Alil L.-C., et al.: Aspects regarding the use of polyethylene fibers for personal armor. Eastern Michigan University, 2004.
4. Cavallaro P.V.: Soft Body Armor: An Overview of Materials, Manufacturing, Testing, and Ballistic Impact Dynamics, N.U.W.C. Division, Editor. 2011, NUWCD-NPT-TR.
5. Laible R.: Ballistic Materials and Penetration Mechanics (Methods and phenomena, their applications in science and technology), 2012, Elsevier.
6. National Institute of Justice, O.o.J.P., U.S. Department of Justice, Stab Resistance of Personal Body Armor NIJ Standard–0115.00. 2000, US National Institute of Justice: Washington.
7. EMS1, Man accused of stabbing 2 police officers after killing 4 relatives. 2023.
8. VOA, Stabbing Attack in Tunisia, Suspect Detained 2022.
9. Staff T.: Police officer stabbed, 10 arrested at Tel Aviv protest over hit-and-run case, in The Times of Israel, 2023.
10. Jessup S., Kelly J.W.: Met Police officer speaks of ordeal as knife attacker is sentenced, in BBC News, 2023, BBC.
11. Amara T.: Tunisia national guard officer stabbed, police arrest attacker, R. Chang, Editor, 2023, Reuters.
12. Police1, N.M. officer killed in stabbing before suspect is shot and killed by witness. 2024, Associate Press.
13. Grieshaber K.: Stabbing attack at German gym leaves 4 severely injured, in Associate Press, 2023, AP.
14. zdfheute, Angriffe auf Bahn-Mitarbeiter 2022 gestiegen. 2023, Panorama.
15. Bundeskriminalamt(BKA), Bundeslagebild Gewalt gegen Polizeivollzugsbeamtinnen und Polizeivollzugsbeamte 2020. 2021, Bundeslagebild.
16. LaTourrette T.: The life-saving effectiveness of body armor for police officers. J Occup Environ Hyg, 7(10), 2010, pp. 557-562.
https://doi.org/10.1080/15459624.2010.489798
17. Peleg K., Rivkind A., Aharonson-Daniel L.: Does body armor protect from firearm injuries? J Am Coll Surg, 202(4), 2006, pp. 643-648.
https://doi.org/10.1016/j.jamcollsurg.2005.12.019
18. Jaslow C.R.: Mechanical properties pf cranal sutures. Journal of Biomechanical, 23(4), 1990, pp. 313-321.
https://doi.org/10.1016/10.1016/0021-9290(90)90059-c
19. Larsen B., et al.: Body armor, performance, and physiology during repeated high-intensity work tasks. Mil Med, 177(11), 2012, pp. 1308-1315.
https://doi.org/10.7205/milmed-d-11-00435
20. Greaves I.: Military Medicine in Iraq and Afghanistan: A Comprehensive Review. 2018, Taylor & Francis Group, CRC Press.
21. Ricciardi R., Deuster P.A., Talbot L.A.: Metabolic Demands of Body Armor on Physical Performance in Simulated Conditions. MILITARY MEDICINE, 173(9), 2008, 817 p.
https://doi.org/10.7205/milmed.173.9.817
22. Park H., et al.: Impact of ballistic body armour and load carriage on walking patterns and perceived comfort. Ergonomics, 56(7), 2013, pp. 1167-1179.
https://doi.org/10.1080/00140139.2013.791377
23. Chinevere T.D., et al.: Efficacy of body ventilation system for reducing strain in warm and hot climates. Eur J Appl Physiol, 103(3), 2008, pp. 307-314.
https://doi.org/10.1177/0040517517690623
24. Nayak R., et al.: Body armor for stab and spike protection, Part 1: Scientific literature review. Textile Research Journal, 88(7), 2017, pp. 812-832.
https://doi.org/10.1177/0040517517690623
25. Nayak R., et al.: Stab resistance and thermophysiological comfort properties of boron carbide coated aramid and ballistic nylon fabrics. The Journal of The Textile Institute, 110(8), 2018, pp. 1159-1168.
https://doi.org/10.1080/00405000.2018.1548800
26. Matusiak M.: Thermal Comfort Index as a Method of Assessing the Thermal Comfort of Textile Materials FIBRES & TEXTILES in Eastern Europe, 18(2), 2010, pp. 45-50.
27. Djongyang N., Tchinda R., Njomo D.: Thermal comfort: A review paper. Renewable and Sustainable Energy Reviews, 14(9), 2010, pp. 2626-2640.
https://doi.org/10.1016/j.rser.2010.07.040
28. Nayak R., et al.: Comfort properties of suiting fabrics. Indian Journal of Fibre and Textile, 34, 2009, pp. 122-128.
29. Philippe F., et al.: Tactile Feeling: Sensory Analysis Applied to Textile Goods. Textile Research Journal, 74(12), 2004, pp. 1066-1072.
https://doi.org/10.1177/004051750407401207
30. Dempsey P.C., Handcock P.J., Rehrer N.J.: Impact of police body armour and equipment on mobility. Appl Ergon, 44(6), 2013, pp. 957-961.
https://doi.org/10.1016/j.apergo.2013.02.011
31. Legg S.J.: Influence of body armour on pulmonary function. Ergonomics, 31(3), 1988, pp. 349-353.
https://doi.org/10.1080/00140138808966679
32. Li Y., Ortiz C., Boyce M.C.: Bioinspired, mechanical, deterministic fractal model for hierarchical suture joints. Phys Rev E Stat Nonlin Soft Matter Phys, 85(3 Pt 1), 2012, 031901 p.
https://doi.org/10.1103/PhysRevE.85.031901
33. Pritchard J., Scott J., Girgis G.: The structure and development of cranial and facial sutures. Journal of Anatomy, 90(1), 1956, pp. 73-86.
34. Herring S.W.: Mechanical influences on suture development and patency. Front Oral Biol, 12, 2008, pp. 41-56.
https://doi.org/10.1159/000115031
35. Dunlop J.W.C., Weinkamer R., Fratzl P.: Artful interfaces within biological materials. Materials Today, 14(3), 2011, pp. 70-78.
https://doi.org/10.1016/S1369-7021(11)70056-6
36. Vernerey F.J., Barthelat F.: On the mechanics of fishscale structures. International Journal of Solids and Structures, 47(17), 2010, pp. 2268-2275.
https://doi.org/10.1016/j.ijsolstr.2010.04.018
37. Dastjerdi A.K., Barthelat F.: Teleost fish scales amongst the toughest collagenous materials. J Mech Behav Biomed Mater, 52, 2015, pp. 95-107.
https://doi.org/10.1016/j.jmbbm.2014.09.025
38. Zhu D., et al.: Puncture resistance of the scaled skin from striped bass: collective mechanisms and inspiration for new flexible armor designs. J Mech Behav Biomed Mater, 24, 2013, pp. 30-40.

https://doi.org/10.1016/j.jmbbm.2013.04.011

39. Lin Y.S., et al.: Mechanical properties and the laminate structure of Arapaima gigas scales. J Mech Behav Biomed Mater, 4(7), 2011, pp. 1145-1156. https://doi.org/10.1016/j.jmbbm.2011.03.024

40. Connors M.J., et al.: Three-dimensional structure of the shell plate assembly of the chiton Tonicella marmorea and its biomechanical consequences. J Struct Biol, 177(2), 2012, pp. 314-328. https://doi.org/10.1016/j.jsb.2011.12.019

41. Ji B., Gao H.: Mechanical properties of nanostructure of biological materials. Journal of the Mechanics and Physics of Solids, 52(9), 2004. https://doi.org/10.1016/j.jmps.2004.03.006

42. Barthelat F., et al.: On the mechanics of mother-of-pearl: A key feature in the material hierarchical structure. Journal of the Mechanics and Physics of Solids, 55(2), 2007, pp. 306-337. https://doi.org/10.1016/j.jmps.2006.07.007

43. Krauss S., et al.: Mechanical Function of a Complex Three-Dimensional Suture Joining the Bony Elements in the Shell of the Red-Eared Slider Turtle. Advanced Materials, 21(4), 2009, pp. 407-412. https://doi.org/10.1002/adma.200801256

44. Garcia A.P., Pugno N., Buehler M.J.: Superductile, Wavy Silica Nanostructures Inspired by Diatom Algae. Advanced Engineering Materials, 13(10), 2011, pp. B405-B414. https://doi.org/10.1002/adem.201080113

45. Martini R., Balit Y., Barthelat F.: A comparative study of bio-inspired protective scales using 3D printing and mechanical testing. Acta Biomater, 55, 2017, pp. 360-372. https://doi.org/10.1016/j.actbio.2017.03.025

46. Ahrendt D., et al.: Hybrid material designs by the example of additive manufacturing for novel customized stab protective clothing, in Light Weight Armour Group for Defense and Security. Roubaix, France, 2019, pp. 286-294.

47. Sitotaw D.B., Muenks D., Kebash A.K.: 3D printing applications on textiles: Measurement of air permeability for potential use in stab-proof vests. Journal of Engineered Fibers and Fabrics, 19, 2024, 15589250241232152 p. https://doi.org/10.1177/15589250241232152

48. Markforged. Markforged the Mark Two Desktop 3D Printer. 2019, online: https://markforged.com/mark-two/ [cited 05.04.2020]

49. Langau L.: What is Continuous Fiber Fabrication (CFF)?, in Make Parts Fast, A Design World Resource, 2017.

50. Dean A.: A Review on Markforged Mark Two: the basics of how it works, in DEVELOP3D, 2016, DEVELOP3D: UK, London.

51. Crease A.: 3D Printer Types & Technologies 2019, Markforged.

52. Association of test laboratories for bullet resistant materials and constructions, Test Standard "Stab and Impact Resistance" - Requirements, classifications and test procedures (VPAM KDIW 2004), 2011.

53. Connor S.E.J., Bleetman A., Duddy M.J.: Safety standards for stab-resistant body armour: a computer tomographic assessment of organ to skin distances. International Journal of the Care of the Injured, 29(4), 1998, pp. 297-299. https://doi.org/10.1016/s0020-1383(97)00205-2

54. Su S., et al.: Skin-Liver Distance and Interquartile Range-Median Ratio as Determinants of Interoperator Concordance in Acoustic Radiation Force Impulse Imaging. Journal of Medical Ultrasound, 27(4), 2019, 4 p. https://doi.org/10.4103/JMU.JMU_124_18

55. Shen F., et al.: Impact of skin capsular distance on the performance of controlled attenuation parameter in patients with chronic liver disease. Liver International, 2015, 9 p. https://doi.org/10.1111/liv.12809

56. Sitotaw D.B., et al.: Investigation of Stab Protection Properties of Aramid Fibre-Reinforced 3D Printed Elements. Fibres and Textiles in Eastern Europe, 29(3(147)), 2021, pp. 67-73.

57. Sitotaw D.B., et al.: A Review on the Performance and Comfort of Stab Protection Armor. 22(1), 2022, pp. 96-107. https://doi.org/10.2478/aut-2021-0013